Journal of Power Sources 193 (2009) 1–8

Contents lists available at ScienceDirect

Journal of Power Sources

journal homepage: www.elsevier.com/locate/jpowsour

Proposal for an optimum water management method using two-pole simultaneous measurement

M. Yamauchi [a,*], K. Sugiura [a], T. Yamauchi [a], T. Taniguchi [b], Y. Itoh [c]

[a] Osaka Prefectural College of Technology, Neyagawa, Osaka 5728572, Japan
[b] Eneos Celltech Co., Ltd., Sakata, Oizumi, Ora-gun, Gunma 3700596, Japan
[c] Sanyo Electric Co., Ltd., Hirakata, Osaka 5738534, Japan

ARTICLE INFO

Article history:
Received 22 September 2008
Received in revised form 20 February 2009
Accepted 20 February 2009
Available online 10 March 2009

Keywords:
PEFC
Flooding/plugging phenomena
Water transportation
Two-pole simultaneous measurement

ABSTRACT

Most designers of Polymer Electrolyte Fuel Cells (PEFCs) supply the PEFC with humidified gas to prevent its membrane from drying. Because the steam generated by the electrochemical reaction is added to a humidified supply gas, the steam partial pressure in the cathode channel forces a supersaturated state. Therefore, the PEFC has water management issues, such as flooding and plugging. Many researchers have studied these issues in the cathode side using a visualization technique, and have introduced water repellency processing to the gas channel and GDL (gas diffusion layer) as a solution. However, the flooding/plugging phenomena in the cathode do not occur alone, and are influenced by the flooding/plugging phenomena in the anode channel through the membrane. Moreover, the water transport phenomenon through the membrane is affected by the locations of the flooding/plugging phenomena in each gas channel. Therefore, we aim to examine the water transport phenomenon through the membrane by the two-pole simultaneous image measurement, and to propose an optimum water management method. This work shows that the flooding/plugging phenomena on the anode side are clearly related to water transportation from the cathode side through the membrane.

1. Introduction

In the future, the Polymer Electrolyte Fuel Cell (PEFC) is expected to become a component in distributed power stations, a power unit for cars, etc., because of its high efficiency and low temperature operation. Since a PEFC generally retains good performance characteristics by controlling the wetting of an electrolyte membrane, most PEFC designers supply the PEFC with humidified gas to prevent drying of the membrane. The steam generated by the electrochemical reaction is therefore added to a humidified supply gas, and the steam partial pressure in the cathode channel forces a supersaturated state. Moreover, because most PEFC designers also humidify the anode gas, the steam partial pressure in the anode gas is increased by the consumption of hydrogen in the electrochemical reaction, which also creates a supersaturated state. These supersaturated states create water management issues in the PEFC like flooding, in which condensate blocks the pores of the GDL, and plugging, where condensate blocks a gas channel. Many researchers have studied these issues on the cathode side using a visualization technique [1–5], and have introduced water repellency processing to the gas channel and GDL [6–9] as a solution. In particular, the hydrophilic GDL is the more effective method in reducing water flooding [4,6–8]. The flooding/plugging phenomena are not limited to the cathode alone, but are influenced by the flooding/plugging phenomena in the anode channel through the membrane. Moreover, the water transport phenomenon through the membrane is affected by the locations of the flooding/plugging phenomena in each gas channel. Generally, the gas flow direction in a standard cell is counter-flow, using a serpentine type channel, with each gas inlet located at the top of the cell and each gas outlet located at the bottom of the cell. Thus, if the cell reaction is uniform throughout the entire electrode, the partial pressure of H_2O in the anode gas channel increases from the inlet to the outlet because hydrogen is consumed by the cell reaction. However, the partial pressure of H_2O in the cathode gas channel would also increase from the inlet to the outlet because oxygen is consumed and steam is generated by the cell reaction. Consequently, for the AT–CT (Anode Top–Cathode Top arrangement) location, the water distribution in each gas channel is low at the top of the cell and becomes higher at the bottom of the cell as shown in Fig. 1(a). This means that if the partial pressure of water in each gas channel of both electrodes is nearly identical, transportation of water through the membrane via the H_2O partial pressure difference is minimal. The transport of water through the membrane is instead influenced by the combination of the water distribution of the anode gas channel and cathode gas channel (these com-

* Corresponding author. Tel.: +81 72 821 6401; fax: +81 72 821 0134.
E-mail address: yamauchi@ipc.osaka-pct.ac.jp (M. Yamauchi).

0378-7753/$ – see front matter © 2009 Elsevier B.V. All rights reserved.
doi:10.1016/j.jpowsour.2009.02.078

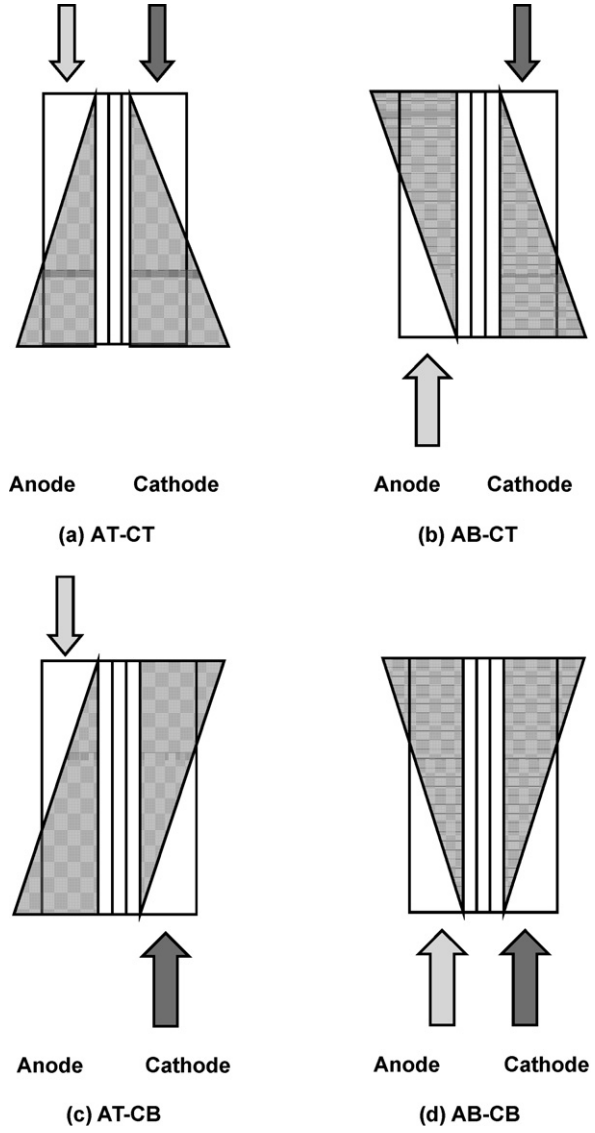

Fig. 1. Combination of anode channel and cathode channel arrangement.

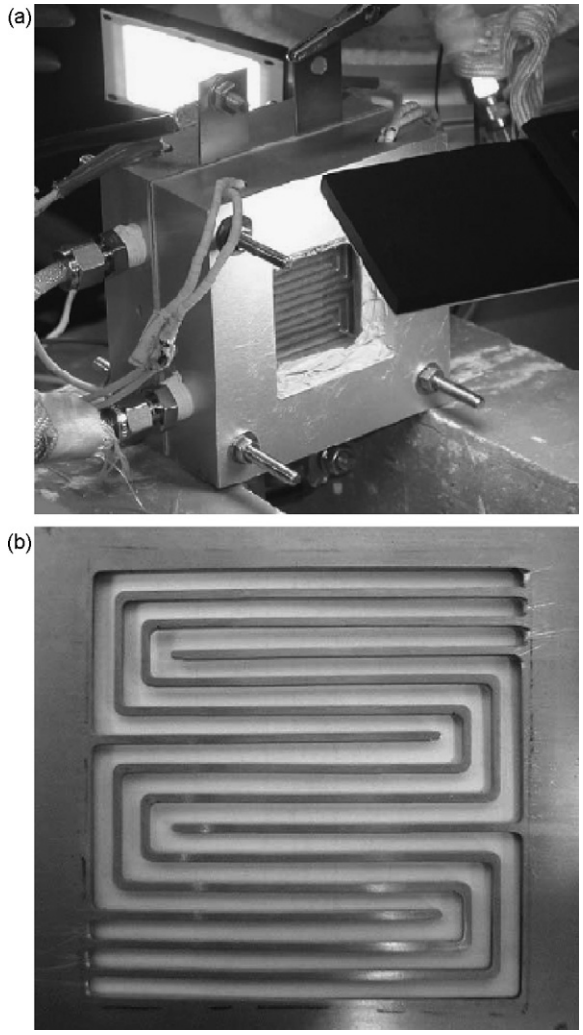

Fig. 2. Photograph of the visualization cell. (a) Photograph of the visualization cell for two-pole simultaneous image measurement and (b) gas channel with the current collector's role.

binations are achieved by the arrangement of each gas inlet), as shown in Fig. 1. The goal of this work is to elucidate the water transport phenomenon through the membrane by two-pole simultaneous image measurement, and to propose an optimum water management method.

2. Experimental cell and apparatus

Fig. 2 shows the visualization cell for two-pole simultaneous measurement and a gas channel with the current collector used as for visualization purposes (Fig. 2(b)). The visualization separator uses a 3-serpentine type channel. Both heater plates of the visualization cell have a quartz observation window. The visualization cell resistance is high, because it includes the visualization separator on both electrodes. The *I–V* performance of visualization cell is therefore worse than that of a non-visualization cell, and both plates are fixed with four M5 screws. The flow field on the anode side is constructed similarly to the cathode flow field. The active cell area is 50 mm × 50 mm. The gas channel has a width of 3 mm, a depth of 1 mm, and a length of 50 mm. The anode catalyst is composed of Pt-Ru/C, and the cathode catalyst of Pt/C. The gas diffusion layer in both electrodes is made of carbon paper (TGPH-060, Toray). The electrolyte membrane is Nafion® 112. This study uses the same MEA (Membrane Electrode Assembly) in all experiments in order to eliminate the influence on the flooding/plugging phenomena caused by the difference in the gas flow direction. Fig. 3 shows the experimental apparatus. The temperature of the PEFC is maintained at 80 °C using a thermoregulator. The anode and cathode gases are passed through a humidifier and then supplied to the PEFC. The piping between the humidifier and the cell is shortened to prevent dew formation in the supply gas, and the piping temperature is maintained by a ribbon heater at 80 °C. Cell voltage is measured and recorded with a data logger. Cell resistance is measured by a milliohm meter with four AC probes. Both channels are irradiated with a metal halide lamp (180 W). The front of

Table 1
Experimental conditions.

Standard condition	Anode	Cathode
Cell temperature (°C)	80	
Gas composition	51 H_2/49 H_2O	51 Air/49 H_2O
Dew point gas humidity (°C)	80	
Gas utilization (%)	70	40
Constant current density (mA cm^{-2})	300	

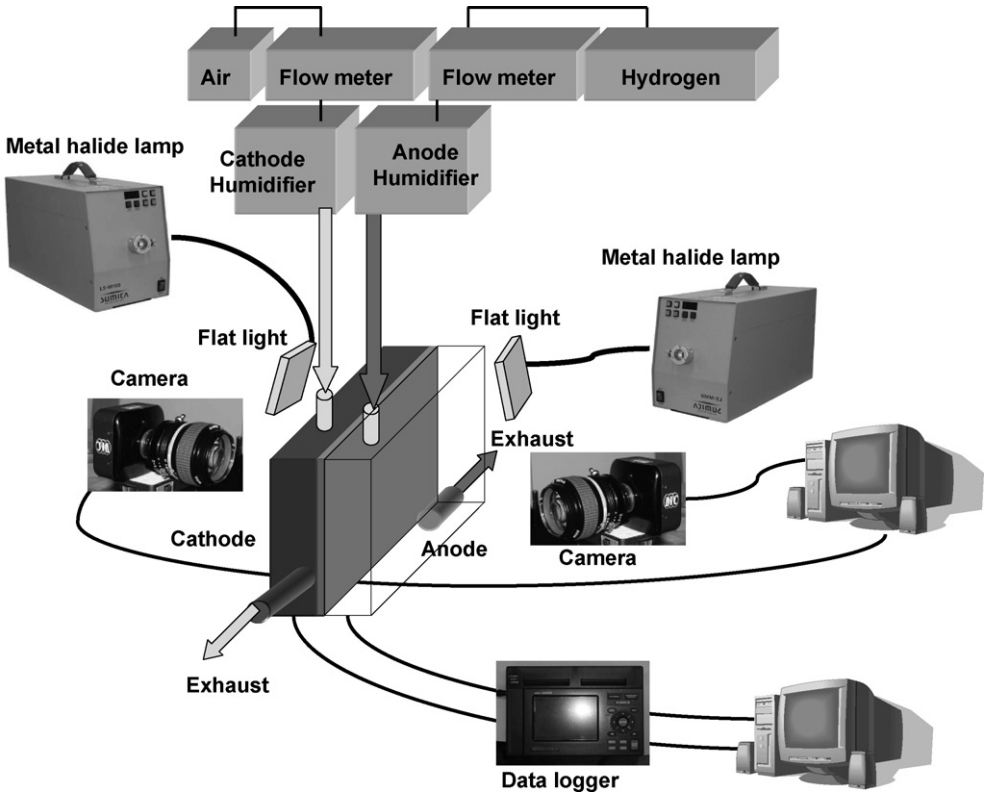

Fig. 3. Schematic diagram of experimental apparatus.

each operating gas channel is imaged with a high spatial resolution video camera (10 bits). Each image has a 1392 pixel (H) × 1040 pixel (V) × 30 fps spatial resolution and is saved directly into the computer memory.

Standard experimental conditions are provided in Table 1. Anode and cathode gases are supplied to the cell through the humidifier at 80 °C. The anode gas composition is 51 H_2/49 H_2O and the cathode gas composition is 51 Air/49 H_2O. Fuel gas utilization is 70%, and oxidant gas utilization is 40%. Though the fuel and oxidant gas utilizations are constant in our experiment, the total amount of the supplied gas increases and decreases because the steam amount varies with the change of each humidifier temperature as shown in Table 2. The *I–V* performance is measured from the change in the OCV (open circuit voltage) to 300 mA cm^{-2} of current density. The cell is driven at a constant current density of 300 mA cm^{-2}, which is the standard in Japan. The operating pressure is atmospheric.

Table 2
Gas compositions of supplied gas with the change of each humidifier temperature.

Humidity temperature [°C]	Gas composition (%)			
	Anode		Cathode	
	H_2	H_2O	Air	H_2O
Anode [30]–Cathode [80]	96	4	53	47
Anode [40]–Cathode [80]	93	7	53	47
Anode [50]–Cathode [80]	88	12	53	47
Anode [60]–Cathode [80]	80	20	53	47
Anode [70]–Cathode [80]	69	31	53	47
Anode [80]–Cathode [80]	53	47	53	47
Anode [80]–Cathode [30]	53	47	96	4
Anode [80]–Cathode [40]	53	47	93	7
Anode [80]–Cathode [50]	53	47	88	12
Anode [80]–Cathode [60]	53	47	80	20
Anode [80]–Cathode [70]	53	47	69	31

3. Results and discussion

3.1. Influence of humidity on the flooding/plugging phenomena in the anode channel

In order to understand the influence of humidity on the flooding/plugging phenomena on the anode side, the performance of a standard cell (AT–CT) was evaluated. Fig. 4 shows *I–V* performance at anode humidifier temperature conditions of 25 °C and 80 °C. Since both *I–V* performance levels are nearly identical, the anode humidity has little influence on the *I–V* performance in this temperature range. Fig. 5 shows images of the anode gas channel as the anode humidifier temperature changes for 300 mA cm^{-2} of current density. Condensate droplets under all humidity conditions, and the size of these droplets increase with the anode humidity. These

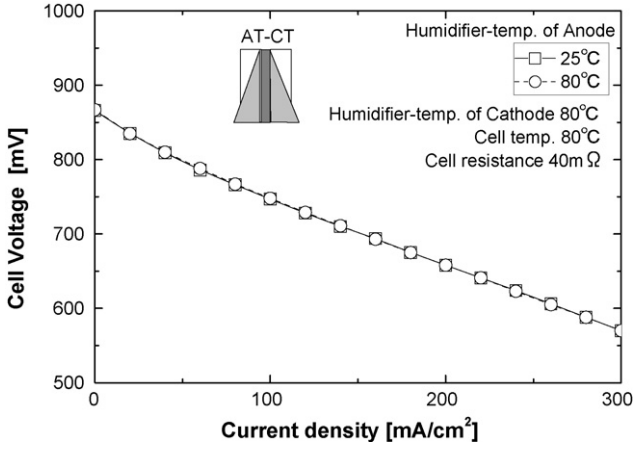

Fig. 4. Influence of anode humidity on *I–V* performance (AT–CT arrangement).

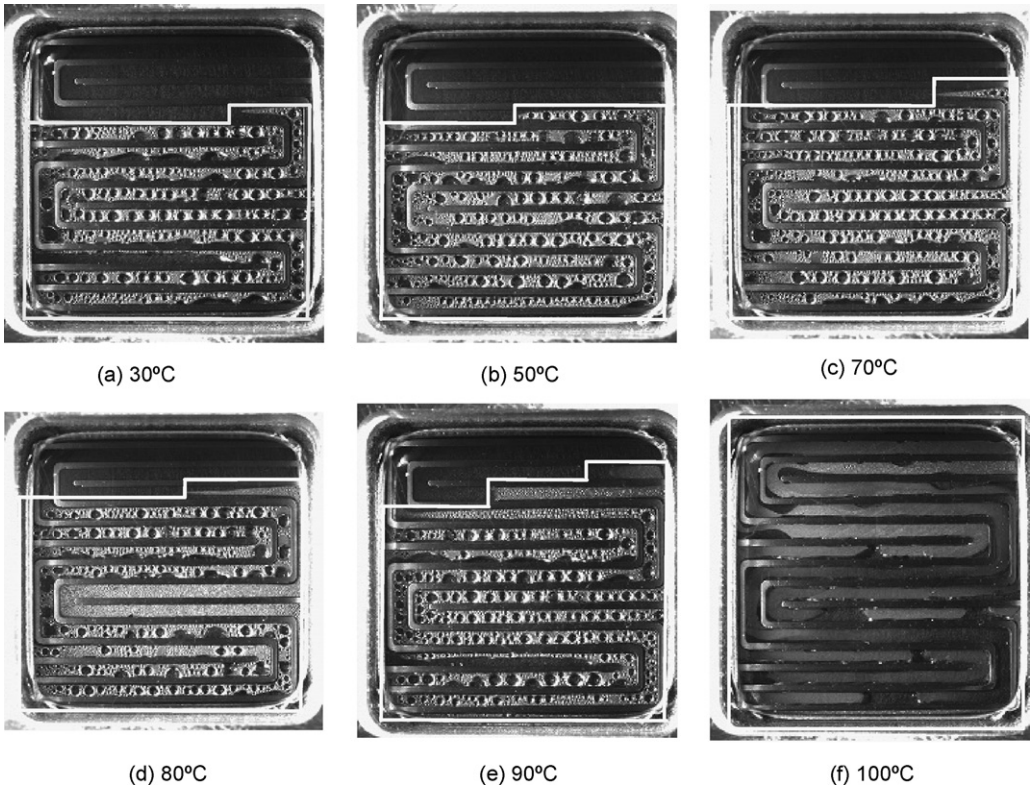

Fig. 5. Measurement images on the anode channel as temperature of the anode humidifier change for 300 mA cm^{-2} of current density (AT–CT arrangement).

droplets may cause plugging if the temperature of the humidifier exceeds 80 °C, with plugging always occurring at 100 °C. However, at 80 °C or less, condensate is rare in the upstream 1/3 section of the anode channel. The condensation rate is defined by dividing the area where the condensate forms by the entire area. Fig. 6 shows the influence of anode humidity on the condensation rate and mean cell voltage. The condensation rate and cell voltage show a large change at 50 °C and 90 °C. Because condensate is present as small droplets until 50 °C as shown in Fig. 5(a) and (b), the supply gas feeds to the electrode with a diffuser effect on the droplets, which adhere to the wall, slightly improving cell voltage, as shown in Fig. 7(a). Thereafter, condensation droplets with the same diameter as the channel width increase in frequency, and the distance between each droplet is also reduced, as shown in Fig. 5(c) and (d). Since the sectional area of the gas channel decreases, as shown in Fig. 7(b), the supply gas flow is constricted and the cell voltage decreases. Plugging is finally caused when these droplets combine, as illustrated in Fig. 5(e) and (f), and the supply gas can barely flow from the plugging point to the outlet, as shown in Fig. 7(c). The cell voltage at 100 °C indicates the minimum where the plugging prevents the reactant gas from reaching the electrode.

In the anode gas channel, condensation does not normally take place under anode humidifier temperature conditions of 60 °C or less even if hydrogen is consumed, and the partial pressure of H_2O increases near the outlet according to the cell reaction. However, experimental results show that the anode gas can be condensed at temperatures as low as 30 °C. Therefore, we understand that the condensation in the anode side is caused by the plugging water on the cathode side being transported to the anode side through the membrane.

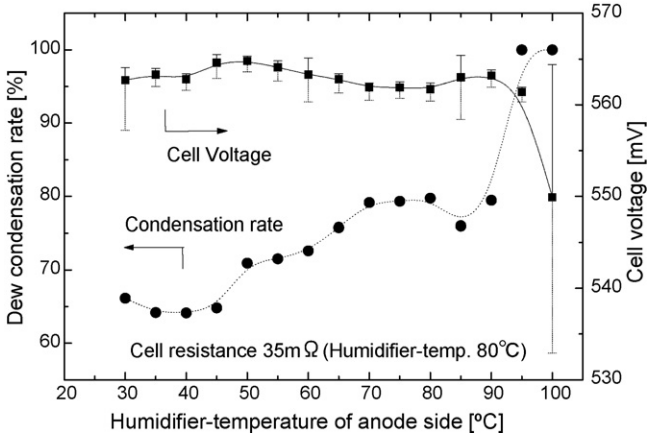

Fig. 6. Influence of anode humidity on the condensation rate and mean cell voltage (AT–CT arrangement).

3.2. Influence of each gas channel arrangement

The water transport phenomenon through a membrane is evaluated by changing the gas channel arrangement, because the plugging phenomenon is influenced by the partial pressure distribution of water in each channel and by gravity. If the gas inlet is installed at the bottom of the cell, the plugging water must exit to the outside against gravity. This combined with the frequent plugging phenomenon at the cathode means it is difficult for the supply gas to sweep the plugging water to the outside. Fig. 8 shows images

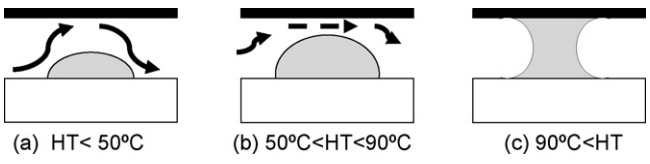

Fig. 7. Schematic diagram of the plugging phenomenon.

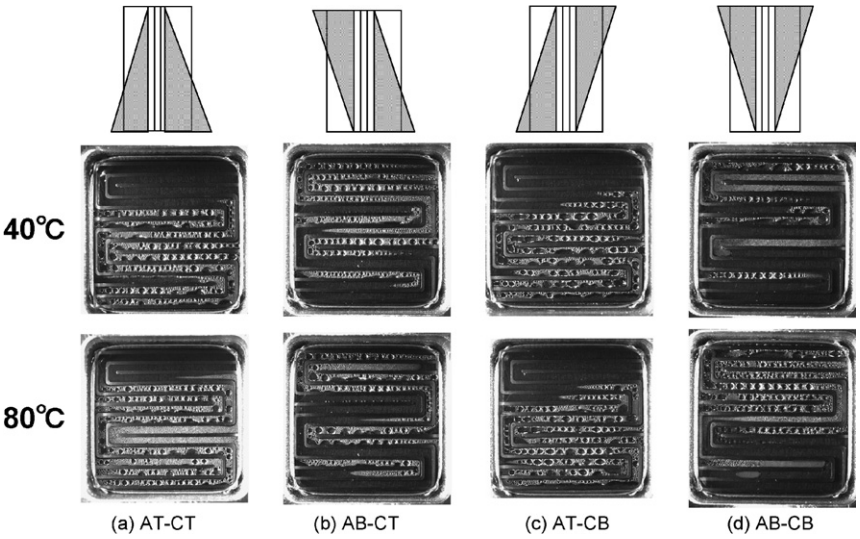

Fig. 8. Measurement images of each gas channel arrangement at 40 °C and 80 °C.

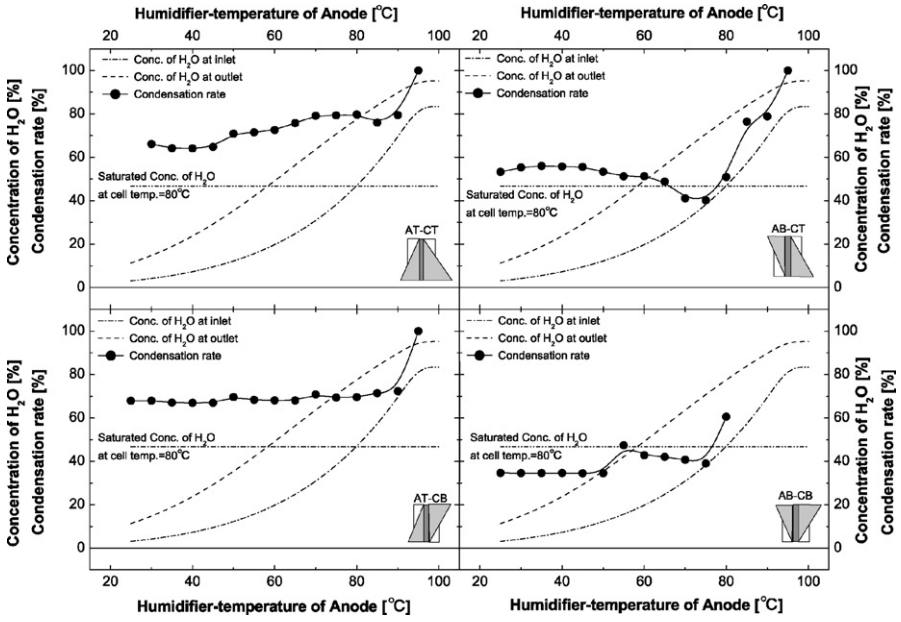

Fig. 9. Influence of each gas channel arrangement on the transport of water.

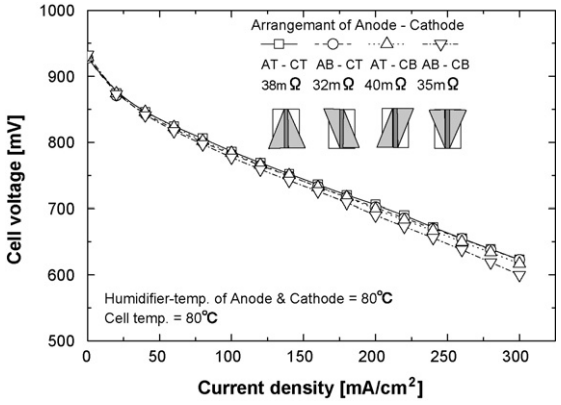

Fig. 10. *I–V* performance of each gas channel arrangement under standard conditions.

on the anode side of each gas channel arrangement at anode humidifier temperatures of 40 °C and 80 °C (the cathode humidifier and the cell temperature remain constant at 80 °C). Fig. 9 shows the influence of each gas channel arrangement on the condensation rate, which is calculated from the measurement images. Fig. 10 shows the *I–V* performance of each gas channel arrangement under standard conditions. In Fig. 9, a broken line indicates H_2O concentration at the anode gas outlet, a dash-dotted line indicates H_2O concentration contained in the supply gas at the anode gas inlet, and a dash-two dotted line indicates the concentration of saturated steam in 80 °C. The concentration of H_2O at the outlet means the gas concentration is a balance of consumed hydrogen via the cell reaction from the supplied anode gas.

The H_2O concentration in the anode gas channel must theoretically be between the dash-dotted line and the dash-two dotted line. If the anode gas humidity does not exceed the humidity that corresponds to the cell temperature, the anode gas is not condensed. Anode gas in all gas channel arrangements is condensed in the region of 50 °C or less, and this region exceeds the range of the H_2O

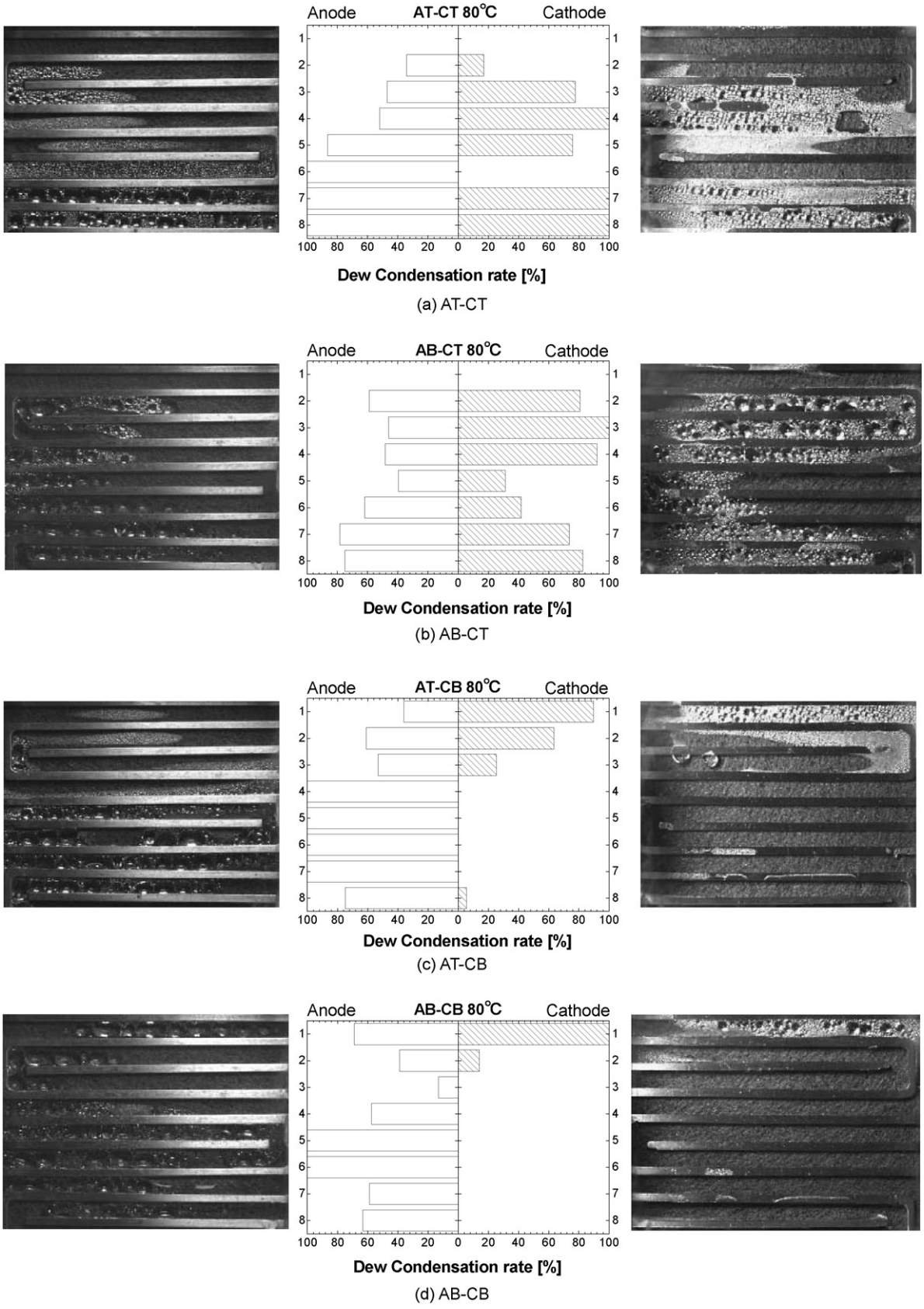

Fig. 11. Water transport phenomenon through the membrane under standard conditions.

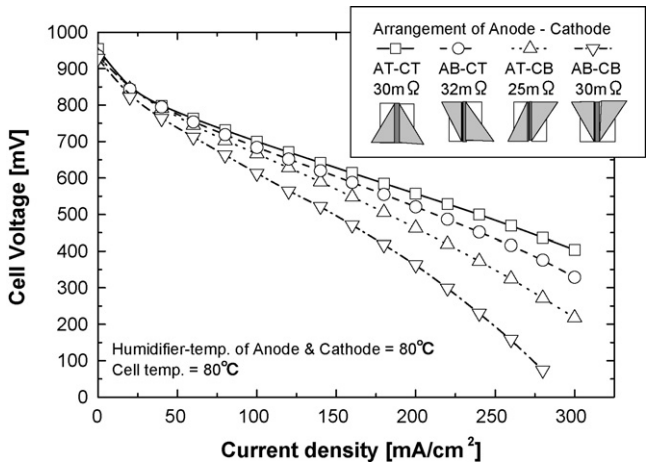

Fig. 12. *I–V* performance of each gas channel arrangement under standard conditions.

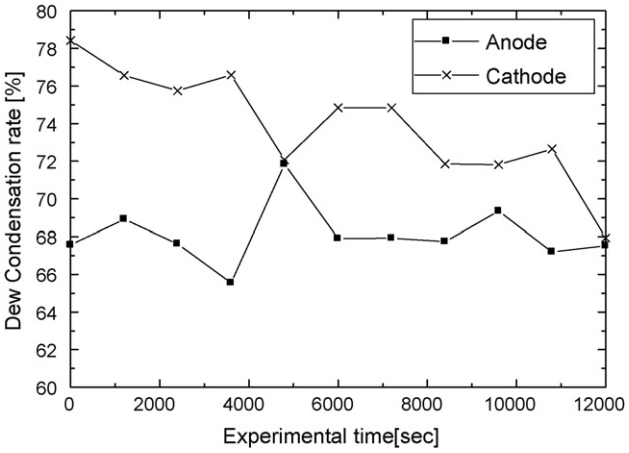

Fig. 14. Dew condensation of AB60–CT80 channel.

concentration in the anode gas channel. Therefore, plugging in this region is caused by water transported from the cathode through the membrane. Moreover, the condensation rates in the anode channel at an arrangement with the anode inlet at the bottom of the cell are lower than that in an arrangement with the anode inlet located in the top of the cell, and that of the AB–CB arrangement is lowest at 70 °C or less. The *I–V* performance of the AB–CB arrangement is also the lowest, as shown in Fig. 10. In the case of the AT–CB arrangement, because the condensation location in the cathode gas channel corresponds to the location without condensation in the anode gas channel, the plugging phenomenon at the cathode is eased by moving water to the anode side through the membrane. This means that although the *I–V* performance of the AT–CB arrangement is improved over that of the AB–CB arrangement, the performance of the CT arrangement is even further improved because the plugging water is easily exhausted to the outside by gravitation.

For the AT arrangement, although plugging water on the anode side is easily exhausted to the outside by gravitation, the condensation rate of the anode side remains high. Since plugging water in the cathode moves to the anode through the membrane, the plugging phenomenon occurs easily in the anode, as shown in Fig. 8(a) and (c), even at low humidity. However, the plugging phenomenon in the cell decreases because the plugging phenomenon in the cathode is eased in the AT arrangement.

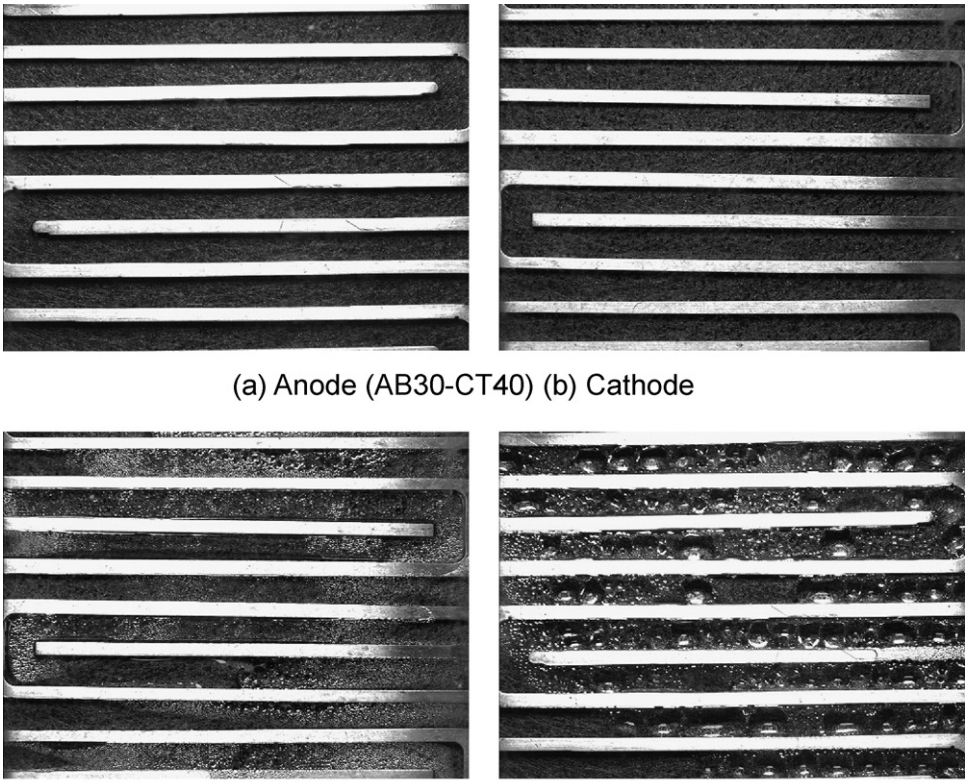

Fig. 13. Measurement image of the channel with changing cathode humidity.

3.3. Verification of water transport phenomenon through the membrane by two-pole simultaneous image measurement

The water transport phenomenon through the membrane mentioned above is verified by simultaneous image measurement of the anode and cathode gas channel. Fig. 11 shows measurement images of each gas channel and the condensation rate of each gas channel under the standard experimental conditions. Here, the cathode image is reversed right to left to make the positions of the anode and the cathode correspond to each other. Each condensation rate corresponds to eight straight channels in each image. Fig. 12 shows the *I–V* performance of each gas channel arrangement under the standard conditions. The *I–V* performance in this figure is worse than that seen in Fig. 10. The cell resistance of this cell is high, because it includes the visualization separator on both electrodes. In Fig. 11, the condensation distribution for all arrangements almost corresponds to the theoretical water distribution shown in Fig. 1. Moreover, the condensation location in the cathode gas channel clearly corresponds to the condensation location in the anode gas channel. However, in the case of the AT–CB and AB–CB arrangements, the condensation on the cathode side does not spread, and the condensation on the anode side spreads throughout the entire area of the gas channel. In particular, the location without condensation in the cathode gas channel clearly corresponds to the condensation location in the anode gas channel in the AT–CB and AB–CB arrangements. The dry part of the cathode occurs because plugging water on the cathode side becomes a film via the influence of gravity and the supply gas pressure, and is then absorbed by the GDL and moves to the anode side through the membrane. This condensation on the anode side creates transport of water from the cathode side through the membrane. The *I–V* performance of the CB arrangement is therefore too poor in terms of flooding the GDL.

However, the *I–V* performance of a conventional arrangement (AT–CT) is high even at high condensation rates. This is because although the plugging phenomenon easily occurs downstream of both gas channels, this plugging water is easily swept away by gravity. In addition, the uniform water distribution in the cell due to the water transportation through the membrane in the AB–CT arrangement makes the *I–V* performance acceptable. If the anode humidity is set low to promote water transportation through the membrane, cell performance will improve more than that of the AT–CT arrangement, and the energy efficiency can be improved by suppressing the energy that makes steam. Therefore, the influences of the humidity of each supply gas stream on water transportation through the membrane must be evaluated by the two-pole simultaneous image measurement technique.

3.4. Plugging water in the cathode moves to the anode through the membrane

In Fig. 9, only anode gas channels are measured to evaluate the influence of each gas channel arrangement. Here, the anode and cathode gas channels of the AB–CT arrangement for cathode humidifier temperatures of 40–80 °C (anode humidifier temperature remains constant at 40 °C) are verified by two-pole simultaneous image measurement, because it is unknown whether the plugging water moves to the anode through the membrane. Fig. 13 shows measurement images of each gas channel at cathode humidifier temperatures of 40 °C and 80 °C (anode humidifier temperature remains constant at 40 °C). Low cathode humidifier temperatures cause poor *I–V* performance in the cell. Plugging water is not observed in any gas channel, as shown in Fig. 13(a) and (b) (AB30–CT40). However, the cell performance does not improve, since the wet membrane means that only the cathode humidifier temperature is elevated. The *I–V* performance for which the cathode humidifier temperature is the same as the cell temperature clearly corresponds to the standard experimental condition, and plugging water is observed in both gas channels as shown in Fig. 13(c) and (d) (AB30–CT80). Results for changing the condensation rates for each of the gas channels in order to supply the optimum water quantity (AB60–CT80) are given in Fig. 14. The condensation rates are synchronized in this case, since the anode condensation rate rises as that of cathode falls. This clearly indicates that plugging water in the cathode moves to the anode through the membrane. Moreover, the cell indicates that the best performance occurs when the humidifier temperature on the anode side is set lower than that on the cathode side, which supplies the optimum water quantity to the cell.

4. Conclusion

The results obtained in this study are summarized as follows.

(1) The flooding/plugging phenomena in the anode gas channel occur in low humidity when water is transported from the cathode to the anode through the membrane.
(2) The condensation in each gas channel occurs at the same location.
(3) The transport of water through the membrane is influenced by the water distribution in each gas channel.
(4) An asymmetrical water-distribution setup, like the AT–CB and AB–CT arrangements, promotes water transport between the two poles.
(5) If anode humidity is set low to promote water transport through the membrane, cell performance of the AB–CT arrangement will improve more than that of a conventional arrangement, and the energy efficiency can be improved by suppressing the energy that makes steam.

Acknowledgements

This work was supported by a Grant-in-Aid for Young Scientists (B) from the Ministry of Education, Science and Culture of Japan (19760126).

Several helpful discussions with Mr. Toshikatsu Kojima of National Institute of Advanced Industrial Science and Technology (AIST) are gratefully acknowledged.

References

[1] K. Sugiura, M. Nakata, T. Yodo, Y. Nishiguchi, M. Yamauchi, Y. Itoh, J. Power Sources 145 (2005) 526–533.
[2] A. Hakenjos, H. Muenter, U. Wittstadt, C. Hebling, J. Power Sources 131 (2004) 213–216.
[3] S. Litster, D. Sinton, N. Djilali, J. Power Sources 154 (2006) 95–105.
[4] K. Tüber, D. Pócza, C. Hebling, J. Power Sources 124 (2003) 403–414.
[5] D. Spernjak, A.K. Prasad, S.G. Advani, J. Power Sources 170 (2007) 334–344.
[6] H. Li, Y. Tang, Z. Wang, Z. Shi, et al., J. Power Sources 178 (2008) 103–117.
[7] G.-G. Park, Y.-J. Sohn, T.-H. Yang, Y.-G. Yoon, J. Power Sources 131 (2004) 182–187.
[8] S. Shimpalee, U. Beuscher, J.W. Van Zee, Electrochim. Acta 52 (2007) 6748–6754.
[9] T. Konomi, T. Kitahara, Y. Iwata, JSME Series B 72 (715) (2006) 207–210 (Japanese).